

DOI: 10.31319/2519-8106.2(49)2023.293111

УДК 539.213.28:541.64

**Kruglyak Irina**<sup>1</sup>, Doctor of Technical Sciences, Professor, Head Department of Mechanical Engineering  
**Кругляк І.В.**, доктор технічних наук, професор, завідувач кафедри галузевого машинобудування  
ORCID: 0000-0001-8872-6778  
e-mail: seredabp@ukr.net

**Baskevich Oleksandr**<sup>2</sup>, Candidate of Physico-mathematical Sciences, Associate Professor,  
**Баскевич О.С.**, кандидат фізико-математичних наук, старший науковий співробітник НДЧ  
Senior Researcher in the Research Unit  
ORCID: 0000-0002-3227-5637

**Gulivets Alexey**<sup>3</sup>, Candidate of Physical and Mathematical Sciences, Associate Professor  
**Гуливець О.М.**, кандидат фізико-математичних наук, доцент  
ORCID: 0000-0003-3410-9605

**Maksimenko Oleg**<sup>1</sup>, Doctor of Technical Sciences, Professor Department of Metallurgy name  
Professor V.I. Loginov

**Максименко О.П.**, доктор технічних наук, професор кафедри металургії ім. проф. В.І.Логінова  
ORCID: 0000-0003-0846-9869

<sup>1</sup>Дніпровський державний технічний університет, м. Кам'янське  
Dniprovsky State Technical University, Kamianske

<sup>2</sup>Український державний хіміко-технологічний університет, м. Дніпро  
Ukrainian State University of Chemical Technology, Dnipro

<sup>3</sup>Український державний університет науки і техніки, м. Дніпро  
Ukrainian State University of Science and Technology, Dnipro

## SIMULATION OF THE STRUCTURE OF CHROMIUM CARBIDE IN THE RESEARCH OF AMORPHOUS ALLOYS

### МОДЕЛЮВАННЯ БУДОВИ КАРБИДА ХРОМУ ПРИ ДОСЛІДЖЕННІ АМОРФНИХ СПЛАВІВ

*Work are considered theoretical aspects of modeling amorphous and nanocrystalline alloys of transition metals and metalloids. Modeling of the close order of amorphous Cr–C alloys obtained by the electrodeposition method was carried out, depending on the current density and temperature of the electrolyte. The dependence between the production conditions and the close order of amorphous alloys was established. A technique for deciphering the radial distribution function of atoms (RDF) based on the concept of the cluster structure of amorphous metals has been developed. Modeling of the close order of amorphous Cr–C alloys was carried out using the approximation of the peaks of FRPA atoms, which are characteristic of the amorphous Ni<sub>86</sub>P<sub>14</sub> alloy. The structure of electrodeposited Cr–C precipitates at different values of current density and electrolyte temperatures was investigated. It was established that the structure of the material is amorphous, and the sizes of the oriented random regions (ORA) vary from 3.6 to 5 nm. The lattice parameters of the samples increase slightly, which is associated with a change in the amount of carbon. The volume of the sediment consists of ORA, the shape of which is close to cuboctahedra, and the volume fraction decreases with an increase in the temperature of the electrolyte.*

**Keywords:** structure modeling, oriented random domains, amorphous alloys, electrodeposition, radial distribution function of atoms.

*У роботі розглядаються теоретичні аспекти моделювання аморфних і нанокристалічних сплавів перехідних металів і металоїдів. Проведено моделювання близького порядку аморфних сплавів Cr–C, які отримані методом електроосадження, в залежності від густини струму та температури електроліту. Встановлено залежність між умовами отримання та близьким порядком аморфних сплавів. Розроблено методику розшифровки функції радіального розподілу атомів (ФРРА) на основі концепції кластерної структури аморфних металів. Проведено моделювання близького порядку аморфних сплавів Cr–C з використанням апроксимації піків ФРРА атомів, що характерні для аморфного сплаву  $Ni_{86}P_{14}$ . Досліджено структуру електроосаджених осадів Cr–C за різних значень густини струму та температур електроліту. Встановлено, що структура матеріалу є аморфною, а розміри орієнтованих випадкових областей (ОВРА) змінюються в межах від 3,6 до 5 нм. Параметри решітки зразків незначно збільшуються, що пов'язано зі зміною кількості карбону. Об'єм осаду складається з ОВРА, форма яких наближена до кубооктаєдрів, а об'ємна частка зменшується зі збільшенням температури електроліту.*

**Ключові слова:** моделювання структури, орієнтовані випадкові області, аморфні сплави, електроосадження, функція радіального розподілу атомів.

### Problem's Formulation

In modern materials science and metallurgy, there is an urgent problem of studying the structure and properties of amorphous and nanocrystalline alloys of transition metals and metalloids, in particular, Cr-C alloys obtained by electrodeposition. Determining the close order of atoms, the conditions for obtaining amorphous phases, and the influence of technological parameters on the structure and properties of alloys is an unsolved problem.

It is necessary to solve the issue of modeling the structure of amorphous alloys at different temperatures and current densities using methods of approximating the peaks of the function of radial distribution of atoms. It is also important to establish the relationship between the conditions of electrodeposition and the close order of amorphous phases, as well as to study changes in the structure and bulk properties of alloys depending on the temperature conditions of production. This will open up new opportunities to improve the production of materials with improved thermal and mechanical properties.

### Formulation of the research goal

The aim of our study is to develop and improve the theoretical basis for modeling the structure of amorphous and nanocrystalline transition metal and metalloid alloys, in particular, Cr-C alloys obtained by electrodeposition. Specific tasks include determining the close order of atoms and their influence on material properties, modeling the structure at different temperature and density conditions of electrodeposition, and establishing dependencies between the conditions of preparation and the close order of amorphous phases. The realization of these tasks will expand our understanding of the properties of amorphous alloys and make a significant contribution to the improvement of technologies for obtaining materials with improved thermal and mechanical characteristics for various industrial applications.

### Presenting main material

The profile of the model peak of the radial scattering function of FRRA atoms in transition metal-phosphorus alloys is determined on the basis of the ideas about the symmetry of the function peaks  $r\rho(r)$ ,  $r^2\rho(r)$  and represented by a Gaussian exponent [1—3]:

$$h_m(r) = A_m \exp \left[ - \frac{(r - r_m)^2}{2\sigma_m^2} \right], \quad (1)$$

whose parameters  $A_m$ ,  $r_m$ ,  $\sigma_m$  are related to the structural characteristics of the system under study, i.e., the average values of coordination numbers, interatomic distances, and relative rms displacements of atoms from the equilibrium position. Depending on specific considerations, the peaks can be approximated by the expressions [1—3]:

$$r\rho(r) = \sum_m B_m \exp\left[-\frac{(r-r_m)^2}{2\sigma_m^2}\right]; \quad (2)$$

$$r^2\rho(r) = \sum_m C_m \exp\left[-\frac{(r-\tilde{r}_m)^2}{2\tilde{\sigma}_m^2}\right]. \quad (3)$$

To determine the parameters of the average values of the coordination numbers, we use the relation (1), which characterizes the  $m$  — coordination sphere and for which we used the approximation of the peaks by the expressions (2—3) [1—3]:

$$Z_m = 4\pi B_m \int_0^\infty r \exp\left[-\frac{(r-r_m)^2}{2\sigma_m^2}\right] \cdot dr = 4\pi B_m r_m \sqrt{2\pi\sigma_m^2}; \quad (4)$$

$$Z_m = 4\pi C_m \int_0^\infty \exp\left[-\frac{(r-\tilde{r}_m)^2}{2\tilde{\sigma}_m^2}\right] \cdot dr = 4\pi C_m \sqrt{2\pi\tilde{\sigma}_m^2}. \quad (5)$$

The average distances between an arbitrary central atom and an atom in the  $m$ th coordination sphere are calculated using the formula:

$$\langle r \rangle = \int_0^\infty 4\pi r^3 \rho(r) dr / \int_0^\infty 4\pi r \rho(r) dr. \quad (6)$$

Then from (6) we obtain:

$$\langle r_m \rangle = r_m \left(1 + \left(\frac{\sigma_m^2}{r_m^2}\right)\right). \quad (7)$$

The latter expression is the most convenient for modeling the apodized FRRA, which can be represented by the relation [1—3]:

$$\begin{aligned} G(r) &= \sum_m \left( \frac{Z_m}{\sqrt{\pi} \cdot r_m} \sqrt{2\sigma_m^2 + 4\pi\tau} \exp(-(r-r_m)^2 / (2\sigma_m^2 + 4\pi\tau)) \right) = \\ &= 4\pi r \rho_0 + \frac{2}{\pi} \int_0^{S_m} (i(s)-1) \cdot s \cdot \exp(-\tau s^2) \cdot \sin(Sr) dS. \end{aligned} \quad (8)$$

Since the sign of the integral (8) includes the square of the exponent, the result of integration is proportional to  $r^2$ , and the FRRA peaks will be close to Gaussian. If (8) is multiplied by  $r$  and the expression proportional to  $r^2$  is used, the model peaks will no longer be Gaussian, and this worsens the approximation of the peaks and, accordingly, the truth of the structure decoding results.

The average distance between an arbitrary central atom and an atom in the  $m$ -coordination layer is given by [1—3]:

$$\langle r_m \rangle = r_m \left(1 + \frac{\sigma_m^2}{r_m^2}\right). \quad (9)$$

The dispersions of the corresponding atomic distances are defined as:

$$u_m^2 = \sigma_m^2 \left(1 - \frac{\sigma_m^2}{r_m^2}\right). \quad (10)$$

When modeling FRRA peaks, it is necessary to take into account the type of relative displacements of atoms from the equilibrium position. It is known that the symmetry of the XRD peaks relative to the maximum position is related to the type of harmonic vibrations of the atoms. If the structural factor is written in the form [1]:

$$i(\vec{s}) = \frac{1}{N} \sum_m \sum_n \langle \exp(i\vec{s}\vec{r}_{mn}) \rangle \langle \exp(i\vec{s}\vec{v}_{mn}) \rangle, \quad (11)$$

and the first factor under the sign of the sums is conserved in all orientations  $\vec{r}_{mn}$  with respect to  $\vec{s}$ , then instead of (11) we have [1]:

$$i(\vec{s}) = \frac{1}{N} \sum_m \sum_n \frac{\sin(sr_{mn})}{sr_{mn}} \langle \exp(i\vec{s}\vec{v}_{mn}) \rangle. \quad (12)$$

Further averaging will be performed taking into account that the vibrations of atoms are harmonic:

$$i(s) = \frac{1}{N} \sum_m \sum_n \frac{\sin(sr_{mn})}{sr_{mn}} \cdot \exp\left[-\frac{1}{4} \left( \frac{s_1^2}{\beta_{mn1}} + \frac{s_2^2}{\beta_{mn2}} + \frac{s_3^2}{\beta_{mn3}} \right)\right], \quad (13)$$

where the conditions of isotropic distribution of relative displacements of atoms are taken into account, at  $\beta_{mn1} = \beta_{mn2} = \beta_{mn3} = \beta_{mn} = \frac{1}{2 \cdot \bar{u}_{mn}^2}$ ,  $\bar{u}_{mn}^2$  — is the root mean square value of the square of the one-dimensional relative displacement of atoms. In this case, we obtain the well-known expression [1]:

$$i(s) = \frac{1}{N} \sum_m \sum_n \frac{\sin(sr_{mn})}{sr_{mn}} \cdot \exp\left(-\frac{\bar{u}_{mn}^2 s^2}{2}\right), \quad (14)$$

where  $s^2 = s_1^2 + s_2^2 + s_3^2$  — is the square of the modulus of the scattering vector.

Let's rewrite expression (14) in a different form, taking into account the same terms:

$$i(s) = 1 + \sum_{m=1}^{\infty} \frac{\sin(sr_{mn})}{sr_{mn}} \cdot \exp\left(-\frac{\bar{u}_{mn}^2 s^2}{2}\right). \quad (15)$$

Relationship (14) is used in the case of linear oscillators. Comparison of expressions (15) and

$i(s) = 1 + \sum_{k=1}^{N-1} Z_k e^{\frac{\sigma_k^2 s^2}{2}} \frac{\sin SR_k}{SR_k}$  allows us to build a model for the function  $P(\vec{x})$  that determines the

probability of the existence of a pair of atoms separated by a radius vector  $\vec{x}$ , or its analog, the function of the radial distribution of atoms  $\rho(\vec{x}) = \frac{N}{V} P(\vec{x})$ . If an object scatters radiation isotropically, then instead of equation (15), its spherical analog should be considered:

$$i(s) = 1 + \frac{1}{s} \int_0^{\infty} 4\pi \cdot x \rho(x) \sin(sx) dx \quad (16)$$

and comparing (15) with (16), we obtain the equation:

$$\int_0^{\infty} 4\pi \cdot x \rho(x) \sin(sx) dx = \sum_{m=1}^{\infty} \frac{Z_m}{r_m} \sin(sr_m) \exp\left(-\frac{\bar{u}_m^2 s^2}{2}\right), \quad (17)$$

whose transformation leads to the relation [4]:

$$G(r) = \frac{1}{\sqrt{2\pi}} \sum_{m=1}^{\infty} \frac{Z_m}{r_m \bar{u}_m} \left\{ \exp\left[-\frac{(r-r_m)^2}{2\bar{u}_m^2}\right] - \exp\left[-\frac{(r+r_m)^2}{2\bar{u}_m^2}\right] \right\}. \quad (18)$$

The contribution of the second term in the curly brackets is insignificant, but this term ensures the symmetry of the function  $rc(r)$  and the coordination peaks  $r_m$  of the isotropic oscillators are symmetrical. The values of the most probable coordination layers are found from the condition of modeling the type of structure of amorphous alloys  $u_m^2$  — from formula (10), and  $Z_m$  — the area of the model peak.

#### **Separation of peaks in the radial distribution function curve.**

The separation of model peaks from the FRRA is possible under certain conditions if the curve consists of visible peaks. Visually, two peaks are separated when a minimum is observed between them [1]:

$$G(r) = \frac{\sin(s_m(r-r_1))}{r-r_1} + \frac{\sin(s_m(r-r_2))}{r-r_2}. \quad (19)$$

Two conditions must  $G(r)$  be met at the minimum point:

$$\frac{dG(r^*)}{dr} = 0, \quad \frac{d^2G(r^*)}{d^2r} < 0, \quad (20)$$

that lead to a claim:

$$\operatorname{tg} \frac{s_m(r_2 - r_1)}{2} \geq \frac{s_m(r_2 - r_1)}{2 - \left[ \frac{s_m(r_2 - r_1)}{2} \right]}, \quad (21)$$

from which it follows that the peaks of function (19) are separated in the best case when the distance between the maxima is equal:

$$r_2 - r_1 > \frac{4,16}{s_m}. \quad (22)$$

The relation (22) is a condition for visual separation of FRRAs peaks of the same height (8), and if the peak heights are different, the resolution will be lower. Reducing the resolution is not the only manifestation of the scattering intensity break effect. The FRRAs peaks also have oscillating wings, the size of which is significant. Thus, if the height of the main maximum of a single peak is equal to one, the depth of the first minimum will be 0.22. In this case, the area of the main peak will be 1.18 times larger than the real coordination number. The shape of the main peak also changes under the influence of overlap with other maxima, and its position also changes.

Since the parameters of the model FRRAs peaks (7) are completely determined by the basic structural characteristics of the atomic system (9—10), it is better to model the FRRAs curve by minimizing the function [5]:

$$Q = \int \{G(r) - G(r)_{\text{ексн}}\}^2 dr \Rightarrow \min, \quad (23)$$

where  $G(r)$  — is the function determined by the FRRAs modeling, and is the  $G(r)_{\text{ексн}}$  FRRAs obtained from the experimental structural factor. As an example, Fig. 1 shows the XRD of the amorphous  $\text{Ni}_{87}\text{P}_{13}$  alloy, approximated by Gaussian peaks (18) to a value of  $r = 1$  nm with a relative error of less than 2 %. This curve is approximated by a set of Gaussian peaks calculated using formula (8), assuming that the OVRAs have a structure close to the HCC.

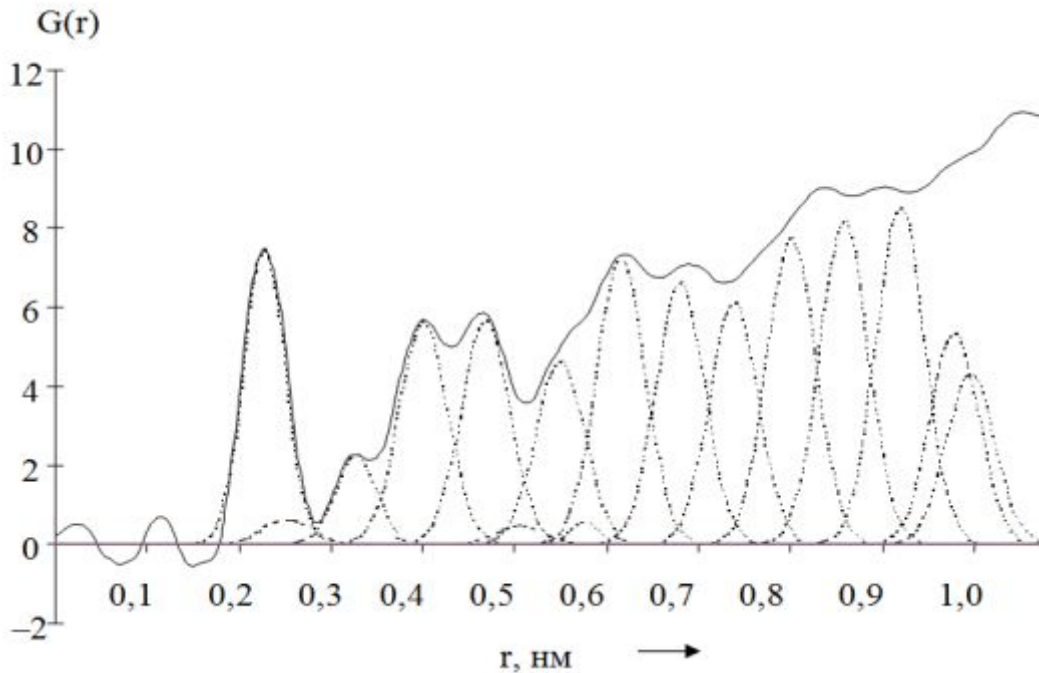


Fig. 1. Approximation by Gaussian peaks of FRRAs  $\text{Ni}_{86}\text{P}_{14}$  at  $\tau = 0,01$ .

As a result of theoretical studies, the influence of basic experimental data on the conditions for modeling the FRA was determined. It was found that the best results are obtained when modeling close-order PM-P alloys by the FRRA using a symmetric Gaussian exponent. At the same time, the FRRA  $G(r)$  (8) is a linear transformation of the true function  $4pc(r)r$  and depends on the basic structural characteristics of the system of atoms.

Using formula (8), the FRRA (Fig. 2) was calculated by the structural factor (Fig. 3) and the type of ordering existing in the Cr-C precipitation was modeled by the peak blurring method. As shown by the simulation data (Tabl. 1), the radii of the first coordination layers for the interatomic distances in nanocrystalline Cr-C alloys are in the range of 0.2471-0.2477 nm, while for crystalline Cr it is equal to 0.250 nm.

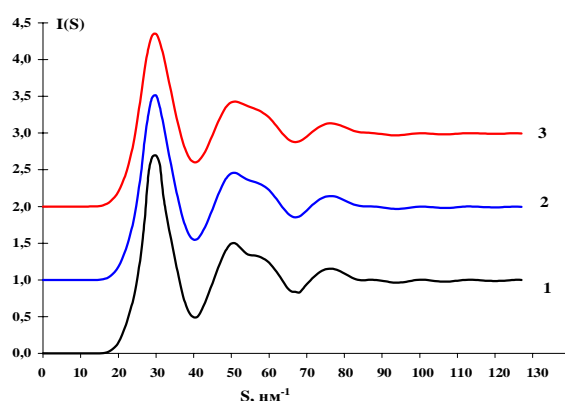


Fig. 2. Structural factors of Cr-C alloys depending on the current density: 1–30 A/дм<sup>2</sup>, 2–35 A/дм<sup>2</sup>, 3–40 A/дм<sup>2</sup>

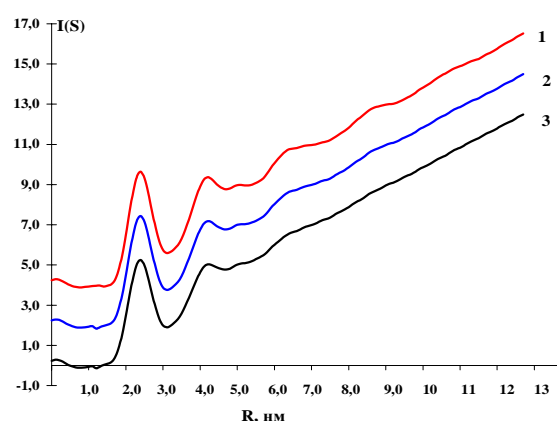


Fig. 3. Function of the radial distribution of Cr-C alloy atoms depending on the current density: 1–30 A/дм<sup>2</sup>, 2–35 A/дм<sup>2</sup>, 3–40 A/дм<sup>2</sup>

Table 1. Close-order decryption data precipitation Cr-C №1–3

| №  | GCC *                             |    |                | №1 Cr <sub>69</sub> C <sub>31</sub> |                |                | №2–Cr <sub>71</sub> C <sub>29</sub> |                |                | №3–Cr <sub>73</sub> C <sub>27</sub> |                |  |
|----|-----------------------------------|----|----------------|-------------------------------------|----------------|----------------|-------------------------------------|----------------|----------------|-------------------------------------|----------------|--|
|    | (r <sub>m</sub> /r <sub>0</sub> ) | Z  | r <sub>m</sub> | (r <sub>m</sub> /r <sub>0</sub> )   | Z <sub>m</sub> | r <sub>m</sub> | (r <sub>m</sub> /r <sub>0</sub> )   | Z <sub>m</sub> | r <sub>m</sub> | (r <sub>m</sub> /r <sub>0</sub> )   | Z <sub>m</sub> |  |
| 1* | 1,000                             | 8  | 0,2477         | 1,000                               | 10,381         | 0,2474         | 1,000                               | 9,521          | 0,2471         | 1,000                               | 9,913          |  |
| 2* | 1,155                             | 6  | –              | –                                   | –              | –              | –                                   | –              | –              | –                                   | –              |  |
| 3* | 1,633                             | 12 | 0,4081         | 1,645                               | 14,149         | 0,4045         | 1,634                               | 12,796         | 0,4050         | 1,639                               | 13,043         |  |
| 4* | 1,914                             | 24 | 0,4738         | 1,912                               | 15,325         | 0,4748         | 1,919                               | 15,109         | 0,4712         | 1,910                               | 16,241         |  |
| 5* | 2,000                             | 8  | –              | –                                   | –              | –              | –                                   | –              | –              | –                                   | –              |  |
| 5  | 2,236                             | 24 | 0,5471         | 2,208                               | 4,084          | 0,5473         | 2,207                               | 22,312         | 0,5491         | 2,225                               | 16,933         |  |
| 6* | 2,309                             | 6  | –              | –                                   | –              | –              | –                                   | –              | –              | –                                   | –              |  |
| 7* | 2,516                             | 24 | 0,6215         | 2,509                               | 24,418         | 0,6200         | 2,505                               | 24,084         | 0,6184         | 2,503                               | 26,632         |  |

where is the coordination number of the crystal structure of the OCC or GCC;

$r_m$  is the radius  $m$  of the coordination sphere.

The first coordination numbers are larger for similar crystal structures, the second and fifth disappear, and the rest differ from integer numbers because, as a result of the high deposition rate and the penetration of carbon atoms into the structure of the chromium matrix, chromium atoms are displaced from equilibrium positions and distort the structure.

Structural factors made it possible to determine the following patterns for samples No. 4–6 of alloys obtained at different electrolyte temperatures (–25°, 2–30°, 3–40°) (Fig. 4) [3].

For samples No. 4–6, similar studies were conducted as for samples No. 1–3 (Figs. 4–5 and Tabl. 2).

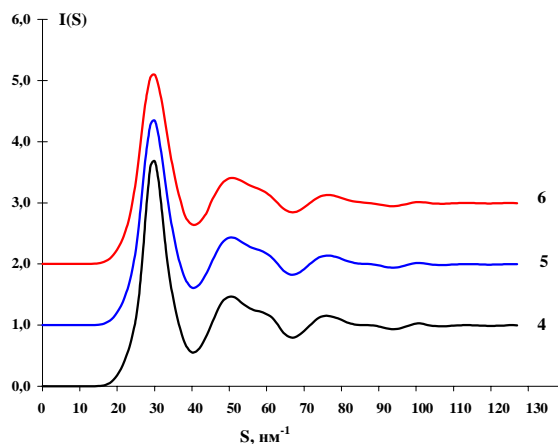


Fig. 4. Structural factors of Cr-C alloys No.4-6 obtained at: 1–25°, 2–30°, 3–40°

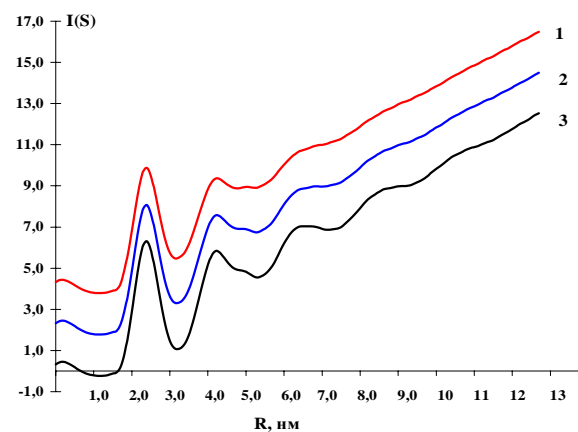


Fig. 5. Function of radial distribution of alloy atoms №4–6 Cr-C: 1–25°, 2 – 30°, 3–40°

Table 2. Close-order decoding data for alloys of samples No. 4—6 Cr-C

| №  | OCC GCC;*   |    | №4 Cr-C |             |        | №5-C-C |             |        | №6-Cr-C |             |        |
|----|-------------|----|---------|-------------|--------|--------|-------------|--------|---------|-------------|--------|
|    | $(r_n/r_0)$ | Z  | $r_n$   | $(r_n/r_0)$ | $Z_n$  | $r_n$  | $(r_n/r_0)$ | $Z_n$  | $r_n$   | $(r_n/r_0)$ | $Z_n$  |
| 1* | 1,000       | 8  | 0,2462  | 1,000       | 10,807 | 0,2465 | 1,000       | 10,593 | 0,2467  | 1,000       | 10,372 |
| 2* | 1,155       | 6  | –       | –           | –      | –      | –           | –      | –       | –           | –      |
| 3* | 1,633       | 12 | 0,4011  | 1,629       | 11,751 | 0,4006 | 1,625       | 11,738 | 0,4018  | 1,628       | 12,101 |
| 4* | 1,914       | 24 | 0,4693  | 1,906       | 20,726 | 0,4710 | 1,911       | 17,502 | 0,4728  | 1,916       | 20,118 |
| 5* | 2,000       | 8  | –       | –           | –      | –      | –           | –      | –       | –           | –      |
| 5  | 2,236       | 24 | 0,5485  | 2,228       | 17,046 | 0,5716 | 2,214       | 19,377 | 0,5491  | 2,225       | 16,933 |
| 6* | 2,309       | 6  | –       | –           | –      | –      | –           | –      | –       | –           | –      |
| 7* | 2,516       | 24 | 0,6117  | 2,509       | 23,202 | 0,6183 | 2,507       | 24,704 | 0,6183  | 2,508       | 24,172 |

The height of the main peak of the structural factor decreases, and its position slightly shifts toward larger angles with increasing electrolyte temperature. At the same time, the heights of the first peaks are higher than in Fig. 4, which means that the crystallinity is higher. The second maxima of the structural factor for Cr-C have different shapes. Thus, the second maxima of the structural factor have a pronounced asymmetric shape with an influx to the left, which slowly decreases with increasing carbon content. Using formula (8), we calculated the FRRA (Fig. 5) and modeled the type of ordering that exists in the OVRAs of Cr-C sediments.

### Conclusions

A methodology for deciphering the FRRA has been developed based on the concept of the cluster structure of amorphous metals and the statement that the OVRAs have the structure of the base metal. The close-order modeling of amorphous Cr-C alloys was performed on the basis of approximation of the peaks of the function of radial distribution of atoms of a typical amorphous alloy Ni<sub>86</sub>P<sub>14</sub>. By modeling the close order of amorphous Cr-C alloys obtained by electrodeposition as a function of current density and electrolyte temperature, the dependence between the conditions of preparation and the close order was established.

It was found that the structure of electrodeposited precipitates obtained at different electric current values and at different electrolyte temperatures is amorphous, with average sizes of the PWAs varying from 3.6 to 5 nm. The lattice parameters of the samples increase slightly, which is associated with a change in the amount of carbon, and the volume of the precipitate consists of OVRAs whose shape is close to cuboctahedra, the volume fraction of which decreases with increasing electrolyte temperature.

### References

- [1] Baskevich, O.S. (2008). Formirovanie amorfnykh splavov perehodnykh metallov s fosforom pri elektroimpulsnom osazhdenii [Formation of amorphous alloys of transition metals with phosphorus during electroimpulse deposition]. *PhD dissertation*, Dnipro National University of Railway Transport named after V. Lazaryan.
- [2] Baskevich, O.S. (2008). Formirovanie amorfnykh splavov perehodnykh metallov s fosforom pri elektroimpulsnom osazhdenii [Formation of amorphous alloys of transition metals with phosphorus during electroimpulse deposition]. *Abstract of PhD dissertation*, Dnipro National University named after Oles Honchar.
- [3] Baskevich, O.S., Hulivetz, A.N., & Zabludovsky, V.O. (2004). Modelirovanie blizhnedejstvuyushih struktur v splavah Ni–P [Modeling of short-range structure in Ni–P alloys]. *Ukrainian Journal of Physics*, 49(12), 1196–1199.
- [4] Hulivets, A.N., Baskevich, A.S., & Shtapenko, E.F. (2000). Modelirovanie struktury amorfnykh plenok Co–P. [Modeling of the structure of Co–P amorphous membrans]. *Visnyk Dnipropetrovskoho Natsionalnoho Universytetu*, 6, 9–14.
- [5] Gulivetz, A.N. (2017). Modelirovanie blizhnego poriadka amorfnykh splavov metall–metalloid [Modeling the short-range order of amorphous metal-metalloid alloys]. *Mathematical Modeling*, 36(1), 78–80.

### Список використаної літератури

1. Баскевич О.С. Формування аморфних сплавів перехідних металів з фосфором при електроімпульсному осадженні: дис. ... канд. фіз.-мат. наук: 01.04.07; Дніпро. нац. ун-т залізн. трансп. ім. В. Лазаряна. – Д., 2008. – 146 с.
2. Баскевич О.С. Формування аморфних сплавів перехідних металів з фосфором при електроімпульсному осадженні [Текст]: автореф. дис. ... канд. фіз.-мат. наук : 01.04.07 / Баскевич О.С. ; Дніпровський національний ун-т ім. Олеся Гончара. – Д., 2008. – 20 с.
3. Baskevich O.S., Gulivetz A.N., Zabludovsky V.O. Modeling of short-range structure in Ni–P alloys. *Ukr. J. Phys.* 2004. V.49, №12. P. 1196–1199.
4. Гуливец А.Н. Баскевич А.С., Штапенко Э.Ф. Моделирование структуры аморфных пленок Co–P. *Вісник Дніпропетровського національного університету. Сер.Фізика. Радіоелектроніка. Дніпро. 2000. №. 6. С. 9–14.*
5. Гуливец А.Н., Баскевич А.С. Моделирование ближнего порядка аморфных сплавов металл–металлоид. *Математичне моделювання. 2017. Т.36(1). С. 78–80.*

Надійшла до редколегії 19.09.2023